

Biosorption Behavior and Reuse Potential of Waste Biomass of *Aspergillus fumigatus*, previously Used in Humic Acid Biosorption, in Removal of Reactive Blue 49

Baoe Wang^{1,2} · Kangqun Zhou¹ · Hui Liu¹ ·
Walter Z Tang²

Received: 23 May 2016 / Accepted: 22 September 2016 / Published online: 5 October 2016
© Springer International Publishing Switzerland 2016

Abstract This study focuses on the reuse of waste biomass after biosorption. The effect of pH on the removal of reactive blue 49 from solution by the waste biomass of *Aspergillus fumigatus*, already used for humic acid biosorption, is studied for the first time in this paper. It is shown that the optimal initial pH was 2.0. The biosorption equilibrium experiment revealed that Langmuir isotherm fits well the biosorption equilibrium data. The theory maximum biosorption capacity was 60.6 mg/g. Kinetic studies indicated that the biosorption process followed the pseudo-second-order kinetics, and that chemisorption might be the rate-limiting step that controlled the biosorption of dye. Thermodynamic studies revealed that the biosorption was a spontaneous exothermic process and that an increased randomness occurred at the solid-solution interface during the fixation of the reactive dyes onto the active sites of the biosorbent. Through chemical modification experiments, it was found that the lipid extraction process for reduction of biosorption capacity was the greatest (17.7 %) compared with the respective 7.1 % and 6.9 % reductions by carboxyl and phosphate groups modified biomass biosorption. This result combined with Fourier transform infrared (FTIR) studies could deduce that lipid took part in the biosorption of reactive blue 49 and occupied a larger proportion among all the biosorption sites. In addition, carboxyl and phosphate groups were the main biosorption functional groups. Thus, it can be proved that the biosorbents can be reused, and still have a good adsorption performance for another adsorbate only if the main biosorption sites in the biosorbent are different.

✉ Walter Z Tang
tangz@fiu.edu

Baoe Wang
baowang@163.com

¹ School of Environmental Science and Engineering, Zhongkai University of Agriculture and Engineering, Guangzhou 510225, China

² Department of Civil and Environmental Engineering, Florida International University, Miami, FL 33172, USA

Keywords Biosorption · Reuse of waste biomass · *Aspergillus fumigatus* · Chemical modification · Biosorption mechanism

1 Introduction

At present, an increasing number of hazardous compounds produced by industries such as mining, metal plating, printing and dyeing, and painting, are being discharged into the water environment. The contaminants come under two broad classes, viz. organic and inorganic. Organic water pollutants include industrial solvents, volatile organic compounds, insecticides, pesticides, dyes, etc. Biodegradation or photo-catalyzed degradation treatments are removal processes for some organic compounds (Karthikeyana et al. 2012; Gupta et al. 2011; Saleh and Gupta 2012b), but their non-degradable byproducts may also be hazardous, and can cause health problems through several channels, such as bioaccumulation (Aksu 2005). Inorganic water pollutants include metals, radioactive substances, fertilizers and acidity (Vijayaraghavan and Yun 2008). Although most are detoxified by physical, chemical and biological treatments before released into the environment, there are still disadvantages in these treatments. For example, the treatment processes for metal and radioactive contaminated waste streams include chemical precipitation (Saleh and Gupta 2012a, b), membrane filtration, ion exchange, carbon adsorption (Gupta et al. 1998) and coprecipitation/adsorption. However, these processes usually require expensive facilities and have high maintenance costs (Chuah et al. 2005).

As a result, biosorption is becoming a promising alternative to replace or supplement the present removal processes of pollutants from wastewaters. Among these pollutants, heavy metals (Farooq et al. 2010; Gupta et al. 2015; Jain et al. 2016), radioactive substances (Bustard et al. 1997), dyes (Hachi et al. 2016), phenolics and pesticides (Aksu 2005), and humic substances (Marija et al. 2008) have been of great concern recently because of their extreme toxicity and/or persistence in the environment. Biosorption of these types of hazardous pollutants by selected live or dead microorganisms, even waste materials, has been investigated by various researchers (e.g., Mittal et al. 2005; Gupta and Nayak 2012; Mittal et al. 2010).

However, the used biosorbents are unavoidably treated as solid waste after several biosorption-desorption cycles, and maximizing reuse of these used biosorbents should be given increased attention. Researches show that many functional groups, such as carboxyl, amino, phosphate and sulfonate, in biomass may contribute to the binding of contaminants (Fu and Viraraghavan 2002). These biosorption sites in the same biosorbent may be different for different biosorbates. As a result, the biosorbents after biosorption of one contaminant may be reused and still have a good biosorption ability of another contaminant, which is a new idea to maximize reuse of biosorbent. In this way, different water treatment departments using the same adsorption process can form an adsorbent recycling chain. Thus, a circular economy is formed among different industries. It is of great significance to promote clean production and circular economy all over the world.

In our previous study, *Aspergillus fumigatus* mycelial pellets were used to adsorb humus (Wang et al. 2013). The study showed that the biomass had a good ability of removal of humus. In this study, the mycelial pellets after biosorption of humic acid were used directly to adsorb reactive blue 49 dye. The biosorption ability, biosorption equilibrium, kinetics, thermodynamics and biosorption sites were examined. The purpose of this study is to prove that biosorbents can be reused, and still have a good adsorption performance for a different adsorbate.

2 Materials and Methods

2.1 Dye and Humic Acid

The anthraquinone dye, C.I. reactive blue 49 (CAS No., 12,236–92-9) (Fig. 1) is an industrial product and was used in the study.

Humic acid, analytical pure, was purchased from Shanghai Huajing bio-hightech Ltd. (Shanghai, China).

2.2 Preparation of Biosorbent

The biosorbent was reused biomass of *Aspergillus fumigatus* after use in biosorption of humic acid. The preparation method was as follows in this study: The *Aspergillus fumigatus* mycelial pellets were harvested after cultured for 72 h in liquid culture medium (Wang and Hu 2007) in conical flasks, and then dried by twist and with filter paper. The dried mycelial pellets were placed in 50 mL of humic acid solution for biosorption in conical flasks on a rotary shaker adjusted at 150 rpm, at biosorption condition of pH 2, temperature of 30 °C, dosage of 2 g/L and humic acid concentration of 25 mg/L. Then, the mycelial pellets adsorbed humic acid were dried in an oven at 60 °C for 12 h. The dried biomass was grinded and sieved through 100 mesh. The powder below the 100 mesh was used as biosorbent.

2.3 Preparation of Humic Acid Solution

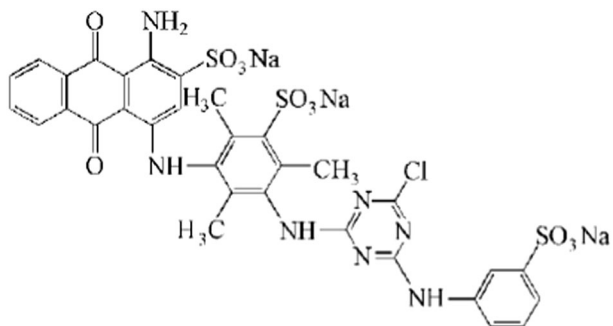
Humic acid (analytical pure, purchased from Shanghai Huajing bio-hightech Ltd., Shanghai, China) was dissolved by NaOH solution at pH 11.0 in order to accelerate dissolution. The supernatant liquid was prepared as a store humic acid solution after filtered through 0.45 μm membrane filters.

2.4 Biosorption Experiments

2.4.1 Effect of Initial pH

The 0.10 g of powder biosorbent was placed in 25 mL reactive blue 49 solution in conical flasks on a rotary shaker adjusted at 150 rpm, 30 °C at dye concentration of 25 mg/L and initial pH range of 2.0 to 11.0 for 1 h. Then, the mixture solution was centrifuged at 3000 rpm for 5 min. The absorbance of supernatant was measured at λ_{\max} 595 nm.

Fig. 1 Chemical structure of reactive blue 49 (the maximum absorption wavelength, λ_{\max} , 595 nm)



2.4.2 Biosorption Kinetics Experiments

The 25 mL reactive blue 49 solution at different concentrations of 56.8 mg/L, 75.3 mg/L, 102 mg/L, 150.9 mg/L and 200.4 mg/L in conical flasks was adjusted to pH 2.0. Then, 0.10 g of powder biosorbent was placed in the dye solutions on a rotary shaker adjusted at 150 rpm, 30 °C, respectively. The liquid samples (10 mL) were taken out at a given time interval for centrifugation at 3000 rpm for 5 min. The absorbance of supernatant was measured at 595 nm.

2.4.3 Thermodynamics Biosorption Experiments

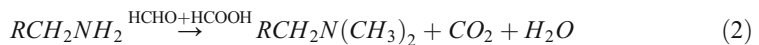
0.10 g of powder biosorbent was placed in 25 mL reactive blue 49 solution in conical flasks on a rotary shaker adjusted at 150 rpm, temperature ranging from 20 °C to 50 °C at dye concentration of 500 mg/L and initial pH 2.0 for 2 h to reach biosorption equilibrium, respectively. Then, the liquid samples (10 mL) were taken out for centrifugation at 3000 rpm for 5 min. The absorbance of supernatant was measured at 595 nm.

2.4.4 Chemical Modification of Biosorbent

Chemical modification of carboxyl: Two g of biosorbent and 1.2 mL of concentrated hydrochloric acid was added to 130 mL of methanol in turn. The mixture was agitated on a rotating shaker at 125 rpm, 22 °C for 6 h. Esterification reaction took place in carboxylic of biosorbent in the process, as follows:



Chemical modification of amino: One gram of biosorbent was added to mixture solution containing of 20 mL formaldehyde and 40 mL formic acid. The mixture was agitated on a rotating shaker at 125 rpm, 22 °C for 6 h. Methylation reaction took place in amino of biosorbent in the process, as follows:



Chemical modification of phosphate group: One gram of biosorbent and 30 mL nitromethane were added to 40 mL triethyl phosphate in turn. After mixing, the mixture was evaporated and refluxed in a water bath pan at temperature range from 80 °C to 90 °C for 6 h. Esterification reaction took place in phosphate of biosorbent in the process.

Lipid Extract One gram of biosorbent was added to 75 mL of acetone, and then the mixture was evaporated and refluxed in a water bath pan at temperature range from 80 °C to 90 °C for 6 h.

2.5 Biosorption Comparison Experiments by Native and Modified Biosorbent

0.10 g of powder original and modified biosorbent were placed into 25 mL reactive blue 49 solution in conical flasks on a rotary shaker adjusted at 150 rpm, 30 °C, at dye concentration of 500 mg/L and initial pH 2.0 for 1 h to reach biosorption equilibrium, respectively. Then, the

liquid samples (10 mL) were taken out for centrifugation at 3000 rpm for 5 min. The absorbance of supernatant was measured at 595 nm. The functional group was analyzed by the comparison of biosorption efficiency of native and modified biosorbent.

2.6 FTIR Spectrum of Native Biomass and Dye-Loaded Biomass

The biomass was separated from the broth by centrifugation after biosorption equilibrium and washed three times with distilled water. Then, the dye-loaded biomass was oven dried (65 °C for 48 h) and grinded as FTIR sample of biomass after biosorption. The infrared spectra of powder of native and dye-loaded biomass samples were measured in a KBr pellet with a Vector 33 Fourier transform infrared spectrometer (Bruker Company, Germany). The wave number was set in the range of 4000 cm^{-1} to 450 cm^{-1} .

2.7 Biosorption Capacity

The biosorption capacity (q) of the reactive blue 49 loading per unit weight of the biosorbent expresses removal extent. The equation for calculation is as follows:

$$q_t = \frac{(C_0 - C_t)V}{m} \quad (3)$$

where q_t is the biosorption capacity at time t (mg/g), V is the volume of biosorption solution, m is the mass of the dry biomass (g), and C_0 and C_t are concentrations of supernatant reactive blue 49 solution before and after biosorption, respectively (mg/L). The values of C_0 and C_t can be calculated by the reactive blue 49 standard curve equation as follows:

$$A = 0.0231C - 0.014 \quad (4)$$

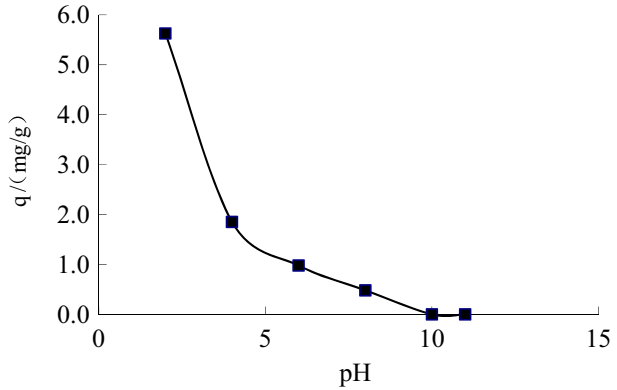
where A is absorbance of reactive blue 49 solution, and C is the dye concentration.

3 Results and Discussion

3.1 Effect of Initial pH

Figure 2 shows the biosorption capacities of reactive blue 49 in initial pH range of 2.0 to 11.0. As shown in Fig. 2, the biosorption capacities decreased with the increase of pH and the best removal observed was 5.6 mg/g at pH 2.0. This indicates that the biosorption is favoured by low pH. Nausheen et al. (2014) studied the removal of Drimarine Yellow HF-3GL dye by sugarcane bagasse, and also observed that the best removal was at pH 2. The observations reveal that electrostatic interaction may be the main mechanism for dye removal by the biosorbent. Reactive blue 49 molecule is amphoteric (shown in Fig.1). The amino molecular structure can be expressed as $\text{H}_3\text{N}^+ - \text{R} - \text{SO}_3\text{Na}$ due to its protonation at low pH solution. As a result, it is positively charged on the surface of the dye. The Zeta potential of mycelial pellets was measured -0.6 mV, which indicates that the biomass is negatively charged due to negatively charged functional groups, such as hydroxyl, carboxyl and phosphate groups. As a result, when the reactive blue 49 contacts with the biosorbent in acid solution, they bind each other quickly by the electrostatic attraction.

Fig. 2 Biosorption capacities of reactive blue 49 at different pH



3.2 Biosorption Kinetics

In the aim of the investigation of the biosorption kinetics, the biosorption capacities of reactive blue 49 were studied at various dye concentrations and for various contact times. The results are shown in Fig. 3. As seen from Fig. 3, the tendency of biosorption capacity variation with contact time at various dye concentrations is similar. That is, the biosorption capacities increased quickly in the first 30 min, and then, they increased more slowly. The greater was the initial dye concentration, the longer equilibrium time was reached. However, in all cases equilibrium was reached within 2 h.

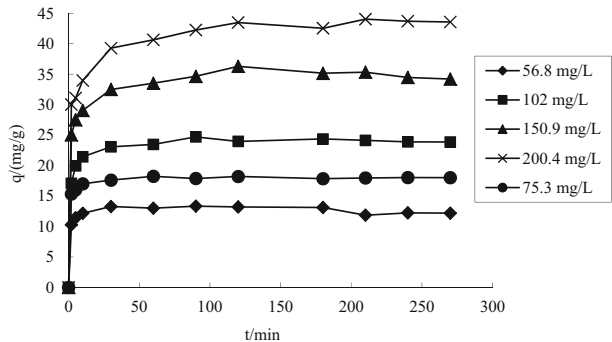
For a comprehensive study of biosorption kinetics characteristics, the most suitable dynamic model should be built. The pseudo-first-order and pseudo-second-order models were used to test adsorption kinetics in this study.

The pseudo-first-order rate expression of Lagergren is given as (McKay and Ho 1999):

$$\log(q_e - q_t) = \log q_e - \frac{k_1}{2.303} t \tag{5}$$

where q_t (mg/g) is the amount of adsorbed dye on the adsorbent at time t , k_1 (min^{-1}) is the rate constant of first-order adsorption, and q_e is the equilibrium sorption uptake. As shown in Table 1, q_e and k_1 were determined from the intercept and slope of the plot of $\log(q_e - q_t)$ versus

Fig. 3 The biosorption capacities of reactive blue 49 at different dye concentrations for different contact time



t, using the data before biosorption equilibrium in Fig. 3 (figure not shown). Table 1 shows that the correlation coefficients are almost all below 0.99, which means that the pseudo-first-order model cannot be used for describing the biosorption kinetics in this study.

The pseudo-second-order kinetic model (McKay and Ho 1999), in its integrated and linearized form, has been used:

$$\frac{t}{q_t} = \frac{1}{k_2 q_e^2} + \frac{1}{q_e} t \tag{6}$$

where k_2 is the rate constant of pseudo-second-order adsorption. As shown in Table 2, q_e and k_2 were determined from the slope and intercept of the plot of t/q_t versus t , using the data before biosorption equilibrium in Fig. 3 (figure not shown).

According to k_2 , the initial biosorption rate h (mg/(g·h)) can be calculated as follows:

$$h = k_2 q_e^2 \tag{7}$$

Table 2 shows that the correlation coefficients are all higher than 0.998. The equilibrium biosorption capacities, q_e , as calculated by the pseudo-second-order kinetic model, increased with the increase of initial dye concentration. The values of the calculated q_e are close to those determined by the experiments. Therefore, it can be concluded that the pseudo-second-order model is suitable to describe the biosorption kinetics of the dyes onto the biosorbent, and that chemisorption might be the rate-limiting step that controls the biosorption of reactive blue 49 (Akkaya and Güzel 2014; Aksu and Çağatay 2006). The values of h are between 14 and 30 mg/(g·min).

3.3 Biosorption Isotherms

Adsorption isotherms can provide information about the optimum use of adsorbents. In this study, the equilibrium data obtained for adsorption were analyzed by using the Freundlich and Langmuir isotherm models. The applicability of the isotherm equations in biosorption was evaluated by using the correlation coefficients, R^2 .

The Freundlich isotherm is an empirical equation based on adsorption on a heterogeneous surface or surfaces supporting varied affinities (Akkaya and Güzel 2014). The linear form of the Freundlich equation is given as:

$$\log q_e = \log K_F + \left(\frac{1}{n}\right) \log C_e \tag{8}$$

Table 1 The pseudo-first-order kinetics model coefficients (k_1 and q_e), and the correlation coefficient R^2

C_0 (mg/L)	Linear equation	k_1 (g/(mg·min))	q_e (mg/g)	R^2
56.8	$y = -0.058x + 0.587$	0.134	3.87	0.997
75.3	$y = -0.023x + 0.438$	0.052	2.74	0.910
102	$y = -0.012x + 0.739$	0.028	5.48	0.974
150.9	$y = -0.0086x + 0.951$	0.020	8.92	0.957
200.4	$y = -0.0115x + 1.105$	0.026	12.75	0.946

Table 2 The pseudo-second-order kinetics model coefficients (k_2 and q_e), initial biosorption rate, and the correlation coefficient R^2

C_0 (mg/L)	Linear equation	k_2 (g/(mg·min))	q_e (mg/g)	h (mg/(g·min))	R^2
56.8	$y = 0.0733x + 0.067$	0.08	13.64	14.90	1
75.3	$y = 0.0546x + 0.033$	0.09	18.32	30.12	1
102	$y = 0.0404x + 0.063$	0.03	24.75	15.77	0.999
150.9	$y = 0.0276x + 0.068$	0.01	36.23	14.75	0.998
200.4	$y = 0.0228x + 0.059$	0.01	43.86	17.92	0.999

where q_e is the equilibrium adsorption capacity (mg/g), C_e is the equilibrium dye concentration (mg/L), K_F is the Freundlich adsorption constant related to adsorption capacity of the adsorbent (L/g), and $1/n$ is the adsorption intensity. The values of K_F and $1/n$ were calculated from the intercept and slope of the plot of $\log q_e$ versus $\log C_e$.

The Langmuir isotherm is based on the assumption that the adsorption process takes place at specific homogeneous sites within the adsorbent surface, and that the adsorption process is monolayer in nature (Akkaya and Güzel 2014).

The linear form of the Langmuir equation is given as:

$$\frac{1}{q_e} = \frac{1}{q_m b} \frac{1}{C_e} + \frac{1}{q_m} \quad (9)$$

In order to determine if the adsorption process is favorable or unfavorable, a dimensionless constant separation factor R_L is used, defined by the following equation:

$$R_L = \frac{1}{1 + bC_0} \quad (10)$$

where b is the Langmuir isotherm constant (L/mg) and C_0 is the initial dye concentration (mg/L). The R_L value indicates whether the type of isotherm is favorable ($0 < R_L < 1$), unfavorable ($R_L > 1$), linear ($R_L = 1$), or irreversible ($R_L = 0$).

As shown in Fig. 4, the biosorption capacities increased with the increase of equilibrium dye concentration. The fitted equation by Langmuir isotherm is as follows:

$$\frac{1}{q_e} = 0.2059 \frac{1}{C_e} + 0.0165 \quad (11)$$

The correlation coefficient R^2 was 0.982. The parameter b was 0.08 L/mg, and the theory maximum biosorption capacity was 60.6 mg/g. As compared with biosorption of dyes by other fungi, this maximum biosorption capacity is not high enough. For example, dye Reactive orange 16 was adsorbed to a maximum of approximately 200 mg/g by *Rhizopus arrhizus* biomass (O'Mahony et al. 2002). The maximum adsorption capacities at 20 °C were calculated to be 160 mg/g for Reactive Blue 19, 122 mg/g for Reactive Red 241 and 137 mg/g for Reactive Yellow 145 by dead macro fungi, namely *Fomes fomentarius* and *Phellinus igniarius* (Zhang et al. 2003). However, the biosorption capacities are not simply comparable due to the different types of dyes. The biosorption capacity is always different for different dyes even

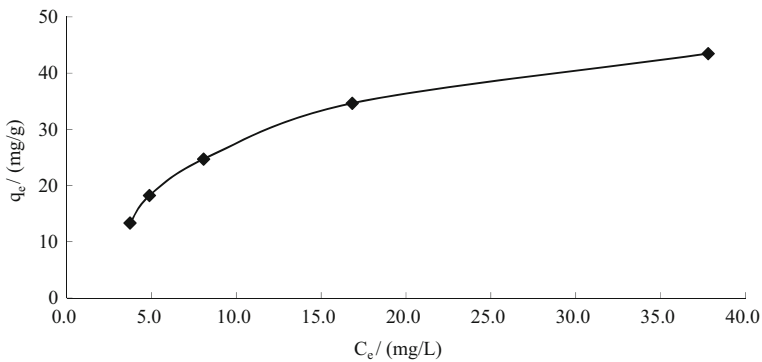


Fig. 4 The equilibrium biosorption capacities at different dye equilibrium concentrations

absorbed by the same biosorbent. Maurya et al. (2006) reported that Methylene Blue (MB) was found to be more adsorbable than Rhodamine Blue (RB). Langmuir monolayer coverage was determined as 204.38–232.73 mg/g and 25.12–36.82 mg/g for MB and RB, respectively.

R_L varied from 0.0587 to 0.1803 according to the different initial dye concentrations, which implies that the Langmuir isotherm is favorable.

The data was also fitted by Freundlich isotherm. The correlation coefficient R^2 was 0.942. The fitted equation by Langmuir isotherm is as follows:

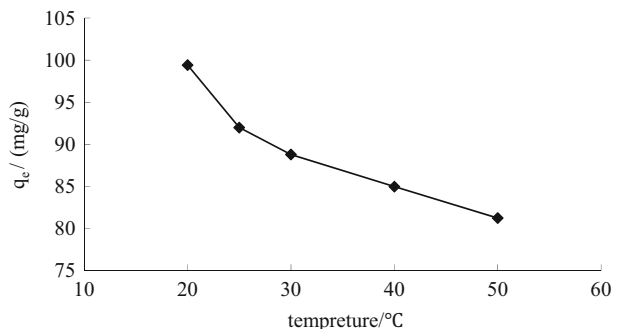
$$\ln q_e = 0.4803 \ln C_e + 2.098 \quad (12)$$

Thus, the high correlation coefficient and R_L values suggest the applicability of the Langmuir model, with the dyes getting adsorbed onto the biosorbent surface to form a monolayer.

3.4 Biosorption Thermodynamics

Figure 5 shows that the biosorption capacity decreased with the increase of temperature. It decreased by 18.18 mg/g for a temperature increase from 20 °C to 50 °C. At higher temperatures, there is increased tendency of the dye molecules to escape from the biosorbent surface into the solution phase, resulting in a decrease in adsorption with increase in temperature. Decreased adsorption at higher temperature also suggests weak interaction between the

Fig. 5 The equilibrium biosorption capacity at different temperatures



biosorbent and the dye molecules, which in turn further supports the physisorption mechanism for dye adsorption (Gupta et al. 2014).

To further evaluate the adsorption process, the thermodynamic parameters were calculated based on the data. The free energy change (ΔG°), enthalpy change (ΔH°), and entropy change (ΔS°) for the adsorption process were calculated using the following equations (Wang et al. 2006; Feng et al. 2011).

$$\Delta G^\circ = -RT \ln K_c \quad (13)$$

$$K_c = \frac{C_{Ae}}{C_e} \quad (14)$$

$$\Delta G^\circ = \Delta H^\circ - T \Delta S^\circ \quad (15)$$

where K_c is equilibrium constant, C_{Ae} is the absorbed dye concentration at equilibrium (mg/L), C_e is the residual dye concentration at equilibrium (mg/L), R is the gas constant (8.314 J/mol·K), T is Kelvin temperature. The values of ΔS° and ΔH° can be obtained by the slope and intercept of ΔG° vs T linear curve, respectively. Table 3 shows the values of the thermodynamics parameters. As seen from Table 3, the thermodynamics parameters were all negative. It can be concluded that the biosorption is exothermic. The negative ΔG° value dictates a spontaneous process. The negative value of ΔS° reveals the increased randomness at the solid-solution interface during the fixation of the reactive dyes onto the active sites of the biosorbent (Gupta et al. 2014).

3.5 Chemical Modification of Biosorbent

In order to determine the main adsorption sites, chemical modification of biosorbent of the carboxyl, amino, phosphate groups and lipids was conducted. The results, also presented in the next section about infrared spectrum analysis, can reveal the role of microcomponents of biomass on the interaction with reactive blue 49.

Figure 6 shows the difference of biosorption capacity of reactive blue 49 by native and chemical modified biomass. It can be seen that the biosorption capacities of chemical modified biomass were all decreased except of amino chemical modification, which instead resulted to a slight increase of biosorption capacity. The decrease of biosorption capacities may be due to the reduction of the number of negatively charged sites on the biomass surface after esterification reaction or acetone treatment (Drake et al. 1996). This reduction could, therefore, reduce the electrostatic attraction of positively charged dye carrying the protonation of amino.

Table 3 Thermodynamics parameters ($R^2 = 0.8599$)

Temperature (K)	ΔG (kJ/mol)	ΔH (kJ/mol)	ΔS (kJ/(mol·K))
293.15	-3.24		
298.15	-2.48		
303.15	-2.26	-16.456	-0.0462
313.15	-1.96		
323.15	-1.66		

Fig. 6 Comparison of biosorption capacity of reactive blue 49 by native and modified biomass

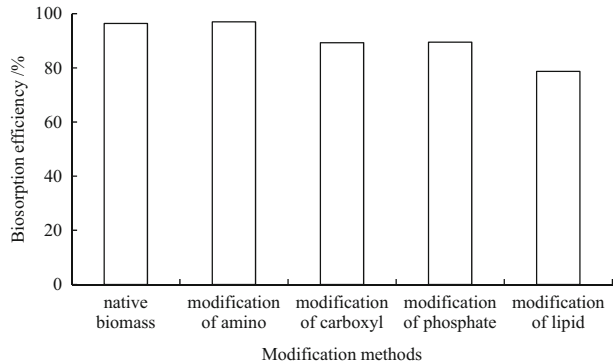


Figure 6 also shows that the lipid extraction process for reduction of biosorption capacity is the greatest, which is 17.7 % compared with the respective 7.1 % and 6.9 % reductions by carboxyl and phosphate groups modified biomass biosorption. This may be due to the hydrophobic interaction between the lipid hydrocarbon chain and hydrophobic groups of the dye molecules. It can also be concluded that lipids take part in the biosorption of reactive blue 49 and occupy a larger proportion among all the biosorption sites. In addition, carboxyl and phosphate groups are main biosorption functional groups.

3.6 FTIR Spectrum of Native and Dye-Loaded Biomass

The FTIR spectra of native and dye-loaded biomass are presented in Figs. 7 and 8, respectively. The spectrum of native biomass (Fig. 7) reveals the presence of carboxylic, amine, and phosphate functional groups, as evident from the broad and strong peak at 3448.2 cm^{-1} ($-\text{OH}$ of carboxylic groups and $-\text{NH}$ of amine groups), the strong peak at 1654.7 cm^{-1} ($-\text{C}=\text{O}$ stretch of carboxyl group and $\text{N}-\text{H}$ bend of amines), and the peak at 1027.9 cm^{-1} ($\text{P}-\text{OH}$ stretch of phosphate group) (Gupta et al. 2014; Won et al. 2006).

Fig. 7 FTIR spectrum of native biomass

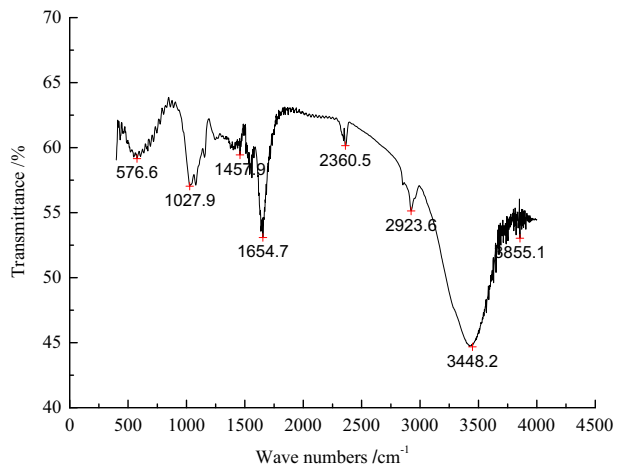
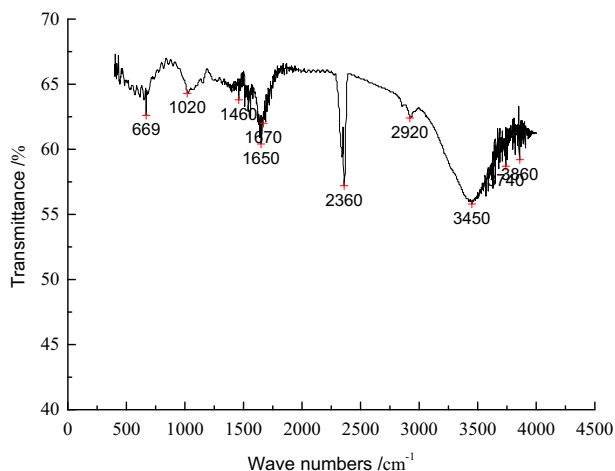


Fig. 8 FTIR spectrum of reactive blue 49 dye-loaded biomass



The comparison of FTIR spectra of dye-loaded biomass with that of native biomass reveals that both peak shapes remained similar, and just some peaks drifted or some vibration intensity weakened or strengthened. This demonstrates that the overall structure of the biosorbent after biosorption is not damaged.

As seen from Figs. 7 and 8, the 3448.2 cm^{-1} peak shifts to 3450 cm^{-1} and the 1654.7 cm^{-1} peak shifts to 1650 cm^{-1} after biosorption of reactive blue 49, respectively, indicating the role of carboxylic groups on biomass surface in the binding process. The apparent reduction of the peak at 1027.9 cm^{-1} to 1020 cm^{-1} reflects the effect of phosphate group on the binding of dyes. In summary, it can be concluded that the carboxylic and phosphate functional groups on the biomass surface have played a great role in biosorption. This conclusion accords with the previous chemical modification experimental result.

In addition, it seems that the amino group in *Aspergillus fumigatus* mycelial pellets was the main group for binding humic acid, while hydroxyl and phosphate groups were involved in the adsorption process in our previous study (Wang and Zhou 2014). This indicates that the main biosorption sites are different for binding humic acid and reactive dyes, respectively. Thus, it seems that the biosorbents can be reused and still have a good adsorption performance for another adsorbate only if the main biosorption sites in the biosorbent are different for the different adsorbates.

4 Conclusions

The following conclusions can be drawn from the study:

- (1) *Aspergillus fumigatus* pellets, previously used in humic acid biosorption, can be reused for dye removal in solutions. The theoretical maximum biosorption capacity was 60.6 mg/g . The acid solution environment is advantageous for biosorption, and the optimal initial pH is 2.0.
- (2) Langmuir isotherm fitted well with biosorption equilibrium data. The biosorption kinetics can be described by pseudo-second-order model, and chemisorption may be the rate-limiting step that controls the biosorption of reactive blue 49. The biosorption is a

spontaneous exothermic process and an increased randomness occurs at the solid-solution interface during the fixation of the reactive dyes onto the active sites of the biosorbent.

- (3) Lipids take part in the biosorption of reactive blue 49 and occupy a larger proportion among all the biosorption sites. In addition, carboxyl and phosphate groups are the main biosorption functional groups.

Acknowledgments The authors are thankful to National Natural Science Foundation committee for providing financial support in the form of project entitled “Biosorption and its mechanism of new reactive dyes by microbiology-humic substance complex” (No. 20807058), and the outstanding young teachers training project funding in institution of higher learning in Guangdong Province (No. Yq2013094). The authors also acknowledge the financial support from the China Scholarship Council.

References

- Akkaya G, Güzel F (2014) Application of some domestic wastes as new low-cost biosorbents for removal of methylene blue: kinetic and equilibrium studies. *Chem Eng Commun* 201:557–578
- Aksu Z (2005) Application of biosorption for the removal of organic pollutants: a review. *Process Biochem* 40: 997–1026
- Aksu Z, Çağatay ŞŞ (2006) Investigation of biosorption of gemazol turquoise blue-G reactive dye by dried *Rhizopus arrhizus* in batch and continuous system. *Sep Purif Technol* 48:24–35
- Bustard M, Donnellan N, Rollan A, McHale AP (1997) Studies on the biosorption of uranium by a thermotolerant, ethanol-producing strain of *Kluyveromyces marxianus*. *Bioprocess Eng* 17:45–50
- Chuah TG, Jumasiah A, Azni I, Katayon S, Thomas Choong SY (2005) Rice husk as a potentially low-cost biosorbent for heavy metal and dye removal: an overview. *Desalination* 175(3):305–316
- Drake LR, Lin S, Rayson GD (1996) Chemical modification and metal binding studies of *Datura innoxia*. *Environ Sci Technol* 30:110–114
- Farooq U, Kozinski JA, Khan MA, Athar M (2010) Biosorption of heavy metal ions using wheat based biosorbents—a review of the recent literature. *Bioresour Technol* 101:5043–5053
- Feng N, Guo X, Liang S, Zhu Y, Liu J (2011) Biosorption of heavy metals from aqueous solutions by chemically modified orange peel. *J Hazard Mater* 185(1):49–54
- Fu Y, Viraraghavan T (2002) Dye biosorption sites in *Aspergillus niger*. *Bioresour Technol* 82:139–145
- Gupta VK, Nayak A (2012) Cadmium removal and recovery from aqueous solutions by novel adsorbents prepared from orange peel and Fe₂O₃ nanoparticles. *Chem Eng J* 180:81–90
- Gupta VK, Srivastava SK, Mohan D, Sharma S (1998) Design parameters for fixed bed reactors of activated carbon developed from fertilizer waste for the removal of some heavy metal ions. *Waste Manag* 17(8):517–522
- Gupta VK, Jain R, Nayaka A, Agarwal S, Shrivastava M (2011) Removal of the hazardous dye—Tartrazine by photodegradation on titanium dioxide surface. *Mater Sci Eng C* 31(5):1062–1067
- Gupta VK, Bhushan R, Nayak A, Singh P, Bhushan B (2014) Biosorption and reuse potential of a blue green alga for the removal of hazardous reactive dyes from aqueous solutions. *Bioremediation. Journal* 18:179–191
- Gupta VK, Nayak A, Agarwal S (2015) Bioadsorbents for remediation of heavy metals: current status and their future prospects. *Environ Eng Res* 20(1):001–018
- Hachi M, Chergui A, Selatnia A, Cabana H (2016) Valorization of the spent biomass of *Pleurotus mutilus* immobilized as calcium alginate biobeads for methylene blue biosorption. *Environ Processes* 3(2):413–430
- Jain CK, Malik DS, Yadav AK (2016) Applicability of plant based biosorbents in the removal of heavy metals: a review. *Environ Processes* 3(2):495–523
- Karthikeyana S, Guptab VK, Boopathya R, Titusa A, Sekarana G (2012) A new approach for the degradation of high concentration of aromatic amine by heterocatalytic Fenton oxidation: Kinetic and spectroscopic studies. *J Mol Liq* 173:153–163
- Marija V, Tomislav D, Felicita B (2008) Removal of humic substances by biosorption. *J Environ Sci* 20:1423–1428
- Maurya NS, Mittal AK, Cornel P, Rother E (2006) Biosorption of dyes using dead macro fungi: effect of dye structure, ionic strength and pH. *Bioresour Technol* 97:512–521
- McKay G, Ho YS (1999) Pseudo-second-order model for sorption processes. *Process Biochem* 34:451–465

- Mittal A, Krishnan L, Gupta VK (2005) Removal and recovery of malachite green from wastewater using an agricultural waste material, de-oiled soya. *Sep Purif Technol* 43(2):125–133
- Mittal A, Mittal J, Malviy A, Gupta VK (2010) Removal and recovery of Chrysoidine Y from aqueous solutions by waste materials. *J Colloid Interface Sci* 344(2):497–507
- Nausheen S, Bhatti HN, Sadaf S, Farrukh Z, Noreen S (2014) Equilibrium modeling of removal of Drimarine yellow HF-3GL dye from aqueous solutions by low cost agricultural waste. *J Chem Soc Pak* 36:177–190
- O'Mahony T, Guibal E, Tobin JM (2002) Reactive dye biosorption by *Rhizopus arrhizus* biomass. *Enzyme Microb Tech* 31(4):456–463
- Saleh TA, Gupta VK (2012a) Column with CNT/magnesium oxide composite for lead(II) removal from water. *Environ Sci Pollut Res* 19(4):1224–1228
- Saleh TA, Gupta VK (2012b) Photo-catalyzed degradation of hazardous dye methyl orange by use of a composite catalyst consisting of multi-walled carbon nanotubes and titanium dioxide. *J Colloid Interface Sci* 371(1):101–106
- Vijayaraghavan K, Yun YS (2008) Bacterial biosorbents and biosorption. *Biotechnol Adv* 26:266–291
- Wang BE, Hu YY (2007) Comparison of four supports for adsorption of reactive dyes by immobilized *Aspergillus fumigatus* beads. *J Environ Sci* 19(4):451–457
- Wang BE, Zhou KQ (2014) Biosorption of humic acid by *Aspergillus fumigatus* mycelial pellets at different conditions and their functional group. 2014 International Conference on Energy and Power Engineering, Hong Kong
- Wang Y, Yang M, Zhao QB, HQ Y (2006) Isotherms, kinetics and thermodynamics of dye biosorption by anaerobic sludge. *Sep Purif Technol* 50(1):1–7
- Wang BE, Zhou KQ, Mai LX, Guo X (2013) Biosorption ability of fulvic acid by *Aspergillus fumigatus* mycelial pellets at different conditions and their interactions during biosorption. *Environ Sci Technol* 36(5):38–42
- Won SW, Choi SB, Yun YS (2006) Performance and mechanism in binding of reactive orange 16 to various types of sludge. *Biochem Eng J* 28:208–214
- Zhang SJ, Yang M, Yang QX, Zhang Y, Xin BP, Pan F (2003) Biosorption of reactive dyes by the mycelium pellets of a new isolate of *Penicillium oxalicum*. *Biotechnol Lett* 25:1479–1482